

FREQUENCY BASED INDUCTIVE RESONANT
WIRELESS POWER TRANSFER FOR MAXIMUM
OUTPUT POWER EFFICIENCY

BY

ISMAIL ADAM

A thesis submitted in fulfilment of the requirement for the
degree of Doctor of Philosophy (Engineering)

Kulliyyah of Engineering
International Islamic University Malaysia

MARCH 2021

ABSTRACT

Wireless Power Transfer (WPT) has been widely used in recent years for charging electric vehicles, powering gadgets, and activating inaccessible wireless devices. With the variety of existing technologies available, the power transferred to wireless electric vehicles, for example, is no longer an illusion. Inductive resonant technology has gained more popularity compared to their counterpart WPT technologies which are inductive and capacitive because it can transfer power over longer distances more effectively and safely. In inductive resonance, the power transferred to the load is maximized if the WPT link has a high-quality factor (Q) and the load impedance is matched properly to the system output impedance provided the WPT link works at the resonance frequency. The main considerations in inductive resonant WPT are to apply the equivalent circuit theory to the model theoretically and analyze the single load inductively coupled WPT system to ensure it works better at the resonance frequency. Therefore, this research focuses on the technique of how the resonance frequency of the inductive resonant WPT link can be estimated. In this research, the possibility of using total harmonic distortion (THD) in finding resonance frequency under varying link impedance conditions, is investigated. An experimental testbed to estimate the resonance frequency of inductive resonant WPT link was developed. Experimental data were obtained by measuring the transmitted and received voltages and then, analyzing them in the offline mode for THD estimates. The results are validated by calculating and comparing WPT performance using experimental data for relative power delivery in resonance, under-resonance, and over-resonance conditions. It has been shown that at the resonance frequency the power delivery reaches the highest point corresponding to the total harmonics distortion at the lowest peak and root mean square voltage (V_{RMS}) of the transmitted voltage (at the primary coil) at the highest peak. This suggests that the resonance frequency estimation of the inductive resonant WPT link can be implemented automatically and dynamically by measuring the transmitted voltage and finding the lowest THD peak and highest V_{RMS} peak using a specially developed algorithm or intelligent system. It is recorded that, at a distance of 0-5cm, the relative power transmitted to the load is increased by 45% at the estimated resonance frequency compared to the relative power delivered to the load at the best-fixed frequency. The result validated that the higher power is transferred to load provided the estimated resonance frequency is closer to the actual resonance frequency. Thus, it proves that it is possible to estimate the resonance frequency of the inductive resonant WPT link by finding the lowest THD value measured on the transmitter side. Therefore, the resonance frequency estimation for inductive resonant wireless power transfer using total harmonics distortion (THD) was successfully explored and employed in this research.

خلاصة البحث

في السنوات الاخيرة تم استخدام تقنية نقل الطاقة اللاسلكية WPT شكل واسع لشحن المركبات الكهربائية وتزويد الاجهزة والمعدات التي لا يمكن الوصول اليها بوسائل سلكية. لم تعد طاقة الرنين الحثي المنقولة لاسلكياً إلى المركبات الكهربائية مجرد وهم بل اكتسبت المزيد من الشعبية مقارنة بالتقنيات المناظرة لها حيث يمكنها نقل الطاقة عبر مسافات أكثر مع المزيد من الفعالية والامان. في تقنية الرنين الحثي يتم نقل أكبر قدرة إذا كان عامل الجودة Q عالي مع تطابق معاوقة الحمل مع معاوقة خرج النظام بشرط ان تعمل عند تردد الرنين. لضمان عمل نظام WPT بشكل أفضل، يجب تحليل النظام المزدوج الأحادي الحمل باستخدام نظرية الدائرة المكافئة لنموذج نظري. لذلك، يركز هذا البحث على كيفية تقدير تردد الرنين لتقنية الرنين الحثي WPT ديناميكياً. في هذا البحث، تم تطوير طريقة استخدام التشوه التوافقي الكلي (THD) في تحديد قيمة تردد الرنين في ظل تغير قيم معاوقة الارتباط المختلفة. كذلك تم تطوير اختبار تجريبي لتحديد قيم تردد الرنين المتغير لتقنية WPT. يتم الحصول على البيانات التجريبية عن طريق قياس الجهد المرسل والمستقبل، وتحليل هذه البيانات في الوضع غير المتصل لتقدير قيمة THD. يتم التحقق من صحة النتيجة من خلال حساب ومقارنة أداء WPT باستخدام البيانات التجريبية للقدرة المرسل لاسلكياً في ظل ظروف أقل من تردد الرنين و تردد الرنين و أعلى من تردد الرنين. من خلال النتائج يتضح انه يتم نقل أعلى قيمة للطاقة عند تردد الرنين في المقابل تكون قيمة التشوه التوافقي الكلي THD عند أدنى جهد ويكون مربع الجهد V_{RMS} للجهد المرسل في الملف الرئيسي عند أعلى قمة. نستنتج من هذا انه يمكن تقدير تردد الرنين عن طريق تحديد أقل قيمة لـ THD و أعلى ذروة للجهد المرسل V_{RMS} . علاوة على ذلك، يشير هذا إلى أنه يمكن تقدير تردد الرنين لوصلة WPT بالرنين الحثي تلقائياً وديناميكياً عن طريق قياس الجهد المنقول وإيجاد أدنى ذروة THD وأعلى ذروة V_{RMS} باستخدام خوارزمية مطورة خصيصاً أو نظام ذكي. تم تسجيل أنه ضمن نطاق 0-4 سم، تزداد الطاقة النسبية المنقولة التي يتم توصيلها إلى الحمل بنسبة 40% عند تردد الرنين المقدر مقارنةً بالقدرة النسبية التي يتم توصيلها إلى الحمل عند أفضل تردد ثابت. يتم تحقيق نقل أعلى قيمة للطاقة المرسل عندما يكون تردد الرنين المقدر أقرب إلى القيمة الفعلية لتردد الرنين. من خلال إيجاد أدنى قيمة THD يكون من الممكن تقدير تردد الرنين لنظام وبالتالي يتم بنجاح ارسال أعلى طاقة ممكنة باستخدام تقنية نقل الطاقة المرسل لاسلكياً WPT وهي من أهم أهداف هذا البحث.

APPROVAL PAGE

The thesis of Ismail Adam has been approved by the following:

Mashkuri Yaacob
Supervisor

Hasmah Mansor
Co-Supervisor

Anis Nurashikin Nordin
Co-Supervisor

Mohamed Hadi Habaebi
Co-Supervisor

Ahmad Fadzil Ismail
Internal Examiner

Ismail Musirin
External Examiner

Mohd Shakir Md Saat
External Examiner

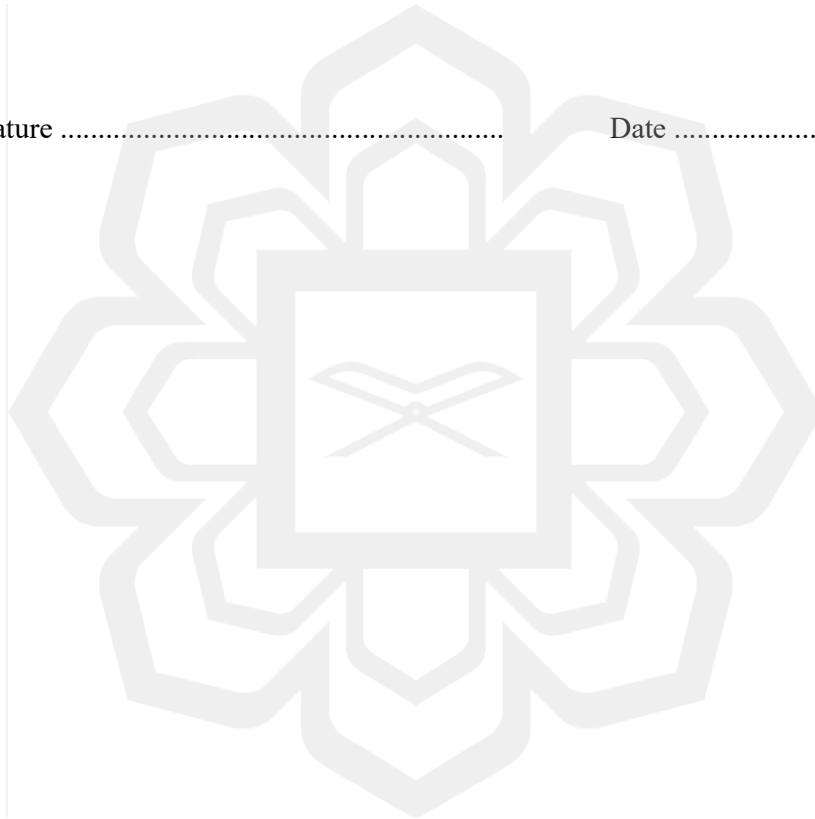
Imad Fakhri Al-Shaikhli
Chairman

DECLARATION

I hereby declare that this thesis is the result of my own investigations, except where otherwise stated. I also declare that it has not been previously or concurrently submitted as a whole for any other degrees at IIUM or other institutions.

Ismail Adam

Signature Date



INTERNATIONAL ISLAMIC UNIVERSITY MALAYSIA

**DECLARATION OF COPYRIGHT AND AFFIRMATION OF
FAIR USE OF UNPUBLISHED RESEARCH**

**FREQUENCY BASED INDUCTIVE RESONANT WIRELESS
POWER TRANSFER FOR MAXIMUM OUTPUT POWER
EFFICIENCY**

I declare that the copyright holders of this thesis are jointly owned by the student and IIUM.

Copyright © 2021 Ismail Adam and International Islamic University Malaysia. All rights reserved.

No part of this unpublished research may be reproduced, stored in a retrieval system, or transmitted, in any form or by any means, electronic, mechanical, photocopying, recording or otherwise without prior written permission of the copyright holder except as provided below

1. Any material contained in or derived from this unpublished research may be used by others in their writing with due acknowledgement.
2. IIUM or its library will have the right to make and transmit copies (print or electronic) for institutional and academic purposes.
3. The IIUM library will have the right to make, store in a retrieved system and supply copies of this unpublished research if requested by other universities and research libraries.

By signing this form, I acknowledged that I have read and understand the IIUM Intellectual Property Right and Commercialization policy.

Affirmed by Ismail Adam

.....
Signature

.....
Date

ACKNOWLEDGEMENTS

First and foremost, praised be to Allah, the Almighty for giving me the patience and guidance throughout this Ph.D. program.

I would like to express my gratitude to my outstanding supervisors, Dato' Seri Professor Dr. Ir. Mashkuri bin Yaacob and Professor Dr. Sheroz Khan, for their great guidance, support, and inspiration throughout this work. My thanks also go to all the co-supervisors for the suggestions and encouragement. Not forgetting, great appreciation to colleagues in Photo Voltage Laboratory, IIUM and Electronics Section, UniKL BMI, for supports and assistance.

Lastly, I would like to thank all my teachers who have done a lot for me, who taught me how to run since I crawled and my students who taught me more than I have taught them, and of course to my parents, wife, and children who have showered me with their loves and supports in all my pursuits. Thanks to all my friends for their constant encouragement.

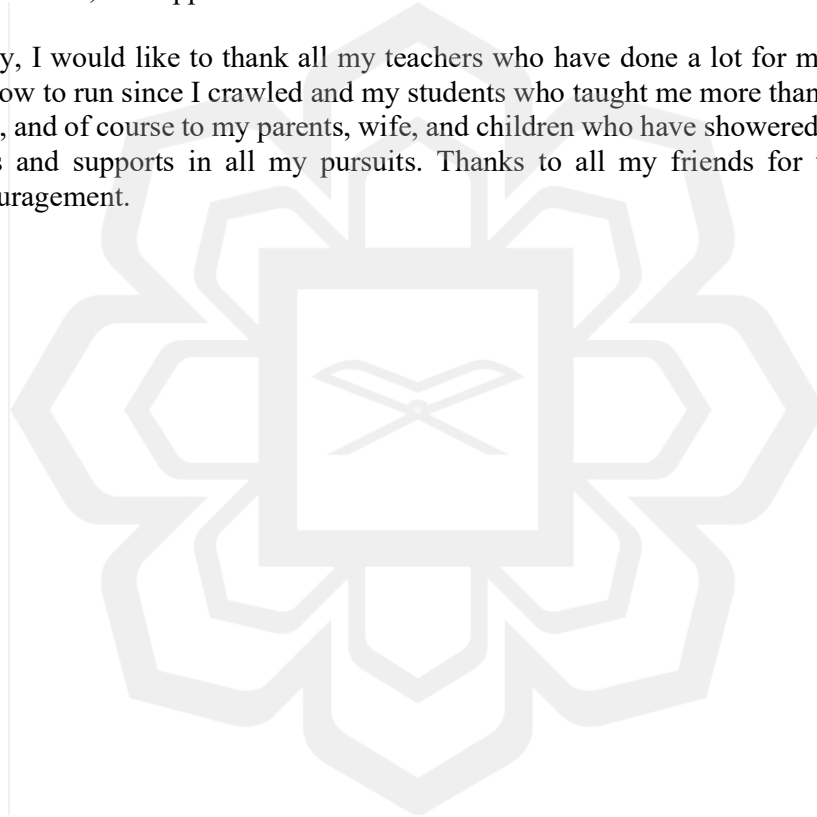


TABLE OF CONTENTS

Abstract.....	ii
Abstract in Arabic	iii
Approval Page.....	iv
Declaration.....	v
Copyright Page.....	vi
Acknowledgements.....	vii
Table of Contents.....	viii
List of Tables	xi
List of Figures	xii
List of Abbreviations	xviii
List of Symbols.....	xix
CHAPTER ONE: INTRODUCTION	1
1.1 Background of Study.....	1
1.2 Research Question	3
1.3 Research Philosophy	3
1.4 Research Hypothesis	4
1.5 Problem Statements	4
1.6 Research Objectives	7
1.7 Research Methodology.....	7
1.8 Scope and Limitation of the Study	10
1.9 Thesis Outline.....	10
CHAPTER TWO: LITERATURE REVIEW	12
2.1 Introduction	12
2.2 Wireless Power Transfer an Introduction.....	12
2.3 Wireless Power Transfer Technology	13
2.4 The Latest Trends in Inductive resonant WPT Research	19
2.4.1 Shape, Geometry, and Material of the WPT Coil.....	21
2.4.2 Impedance Matching Technique.....	22
2.4.3 Coupling Coefficient Estimation	24
2.5 Inductive Resonant WPT Link	27
2.6 Related Theory	30
2.6.1 Conversion to Equivalent T-Network.....	30
2.6.2 Fast Fourier Transform	32
2.6.3 Total Harmonics Distortion (THD).....	33
2.6.4 Composition of the VRMS	33
2.7 Summary.....	34
CHAPTER THREE: RESEARCH METHODOLOGY	35
3.1 Introduction	35
3.2 Research Framework.....	35
3.2 Inductive Resonant Wireless Power Transfer	37
3.3 Input Impedance and Coupling Coefficient Relationship	46
3.4 Load Dependency on Power Efficiency Analysis	48

3.5	Frequency-based Inductive Resonant Wireless Power Transfer	49
3.5.1	Fourier Transform of the Square Wave.....	49
3.5.2	Series-to-series Inductive Resonant WPT Transfer Function	50
3.5.3	Energizing the Transmitting Coil with the Square Wave.....	52
3.5.4	Proposed Frequency-based Inductive Resonant WPT Link.....	56
3.5.5	Hardware Architecture of Proposed Link.....	57
3.5.6	Software Requirement	58
3.6	Project Circuit Schematic Diagram	60
3.6.1	Transmitter Schematic Circuit.....	61
3.6.2	Receiver Schematic Circuit	62
3.6.3	Transmitter Printed Circuit Board	63
3.6.4	Receiver Printed Circuit Board.....	65
3.7	Experimental Design	66
3.7.1	The Overall Flow-chart of the Experimental Circuit.....	67
3.7.1.1	PWM Indicator Sub-block.....	68
3.7.1.2	Pulse Width Modulation Control Sub-block	69
3.7.1.3	Frequency Step Selection Mode Sub-block.....	70
3.7.1.4	Up/Down the Frequency Mode Sub-block.....	70
3.7.2	Validation of Proposed Resonance Estimation Technique	72
3.8	Summary.....	74
CHAPTER FOUR: RESULTS AND DISCUSSION		75
4.1	Introduction	75
4.2	Inductive Resonant Wireless Power Transfer	75
4.3	Input Impedance and Coupling Coefficient Relationship	81
4.4	Load Dependency on Power Efficiency	83
4.5	Resonance Frequency Estimation Analysis.....	89
4.5.1	Use of THD, Crest Factor, and RMS for Signal Estimates	90
4.6	Fix Position and Variable Frequency	98
4.6.1	Experiment 1	98
4.6.2	Experiment 2	103
4.6.3	At a Fix Position	107
4.7	Fix Frequency Variable Position	108
4.7.1	Experiment 3	108
4.7.2	Experiment 4	112
4.7.3	Moving Coil at a Fixed Frequency	115
4.8	Experimental Result at Resonance	116
4.9	THD at Resonance.....	119
4.10	Voltage and Power Delivery.....	120
4.11	Summary.....	124
CHAPTER FIVE: CONCLUSION AND SUGGESTION		126
5.1	Conclusion.....	126
5.2	Significant Contribution of the Research	130
5.3	Suggestion for Future Works.....	131
REFERENCES.....		132

LIST OF PUBLICATIONS 137
APPENDIX A 138
APPENDIX B 140
APPENDIX C 144



LIST OF TABLES

Table 2.1 WPT Technologies, Range, Frequency Range, Coupling Device and Applications	14
Table 3.1 Calculations and Tasks	58
Table 4.1 Average Power Transfer Efficiency for Inductive Resonant WPT	80
Table 4.2 Input Impedance Against the Coupling Coefficient	81
Table 4.3 The Power Transfer Efficiency to the Coupling Coefficient and Load Impedance	86
Table 4.4 The Power Transfer Efficiency to the Coupling Coefficient and Optimum Load Impedance	87
Table 4.5 Values of THD, Crest Factor, and VRMS at Multiple Frequencies	97
Table 4.6 Resonance Frequency and THD to Distance	120
Table 4.7 VRMS (V) Measured at the Load Impedance to Distance	121
Table 4.8 Power (W) Delivered to Coils Distance	121

LIST OF FIGURES

Figure 1.1 Methodology Diagram	9
Figure 2.1 The Concept of the Wireless Power Transfer	14
Figure 2.2 Capacitive Coupling Wireless Power Transfer	15
Figure 2.3 Inductive Coupling Wireless Power Transfer	16
Figure 2.4 Resonant Inductive Coupling Wireless Power Transfer	16
Figure 2.5 Magneto Wireless Power Transfer	17
Figure 2.6 Laser Wireless Power Transfer	17
Figure 2.7 Microwave Wireless Power Transfer	18
Figure 2.8 The Inductance WPT Magnetically Coupled Circuit	27
Figure 2.9 Magnetically Coupled Coils	30
Figure 2.10 Equivalent T-Network	31
Figure 2.11 Magnetically Coupled Circuit	31
Figure 2.12 Magnetically Coupled Circuit Conversion to T-Network	31
Figure 2.13 Eight-Point FFT Flow Graph Using Decimation-In-Frequency	32
Figure 3.1 Research Framework Diagram	36
Figure 3.2 Magnetically Coupled Series-to-Series Configuration	38
Figure 3.3 T-Network Circuit of Series-to-Series Configuration	38
Figure 3.4 T-Network Circuit of Series-to-Parallel Configuration	40
Figure 3.5 Current Across the Load in Series-to-parallel Configuration	41
Figure 3.6 T-Network Circuit of Parallel-to-Series Configuration	42
Figure 3.7 T-Network Circuit of Parallel-to-Parallel Configuration	43
Figure 3.8 Current Across the Load in Parallel-to-parallel Configuration	45
Figure 3.9 MATLAB Simulink Test Bench Model	47

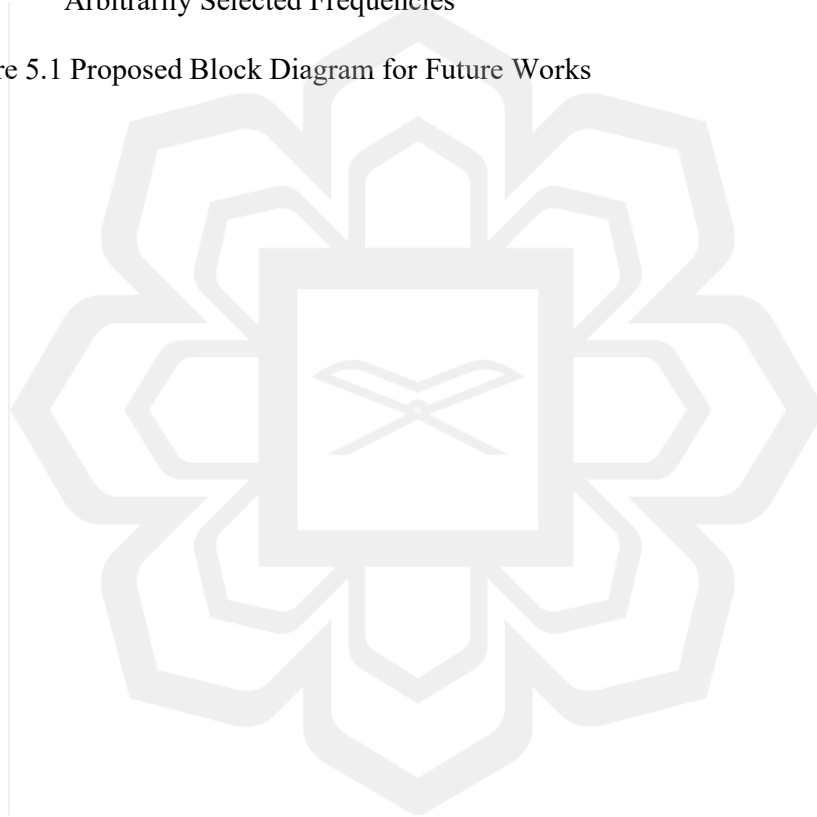
Figure 3.10 DC-to-AC Output Waveform Under Resistive Load	49
Figure 3.11 The Fourier Series of the Square Wave	50
Figure 3.12 Inductive Resonant WPT Magnitude Response	51
Figure 3.13 The Frequency Spectrum of a Square Wave at a Frequency Equal to the Link Cut Off Frequency	52
Figure 3.14 The Frequency Spectrum of Square Wave Affected by Link Frequency Response at Frequency Equal to Link Cut Off Frequency	52
Figure 3.15 The Square Wave Affected by Link Frequency Response at Frequency Equal Link Cut Off Frequency	53
Figure 3.16 The Waveform of Figure 3.15 in the Frequency Domain	53
Figure 3.17 The Frequency Spectrum of Square Wave Affected by Link Frequency Response at Frequency Less Than Link Cut Off Frequency	54
Figure 3.18 The Square Wave Affected by Link Frequency Response at Frequency Less Than Link Cut Off Frequency	54
Figure 3.19 The Waveform of Figure 3.19 in the Frequency Domain	55
Figure 3.20 The Frequency Spectrum of Square Wave Affected by Link Frequency Response at Frequency More Than Link Cut Off Frequency	55
Figure 3.21 The Square Wave Affected by Link Frequency Response at Frequency More Than Link Cut Off Frequency	56
Figure 3.22 The Waveform of Figure 3.21 in the Frequency Domain	56
Figure 3.23 The Proposed Block Diagram of the Frequency-Based Inductive Resonant Wireless Power Transfer	57
Figure 3.24 The Signal Conditioning Sub-block to Sample the Transmitted Voltage	57
Figure 3.25 The Inverter Sub-Block to Drive the Transmitting Coil	58
Figure 3.26 Individual Harmonics Components and Peak Voltage Determination	58
Figure 3.27 Flowchart of the FFT up to 256-point	59
Figure 3.28 Relationship of all the properties i.e., THD, rms, V_p and Crest Factor	60

Figure 3.29 Transmitting Unit Circuit	61
Figure 3.30 3D Looks of the Transmitting Unit	62
Figure 3.31 Receiver Unit Circuit	63
Figure 3.32 The Printed Circuit Board Looks of the Transmitting Unit	64
Figure 3.33 The 3D Looks of the Transmitting Unit	64
Figure 3.34 The Printed Circuit Board Looks of the Receiving Unit	65
Figure 3.35 The 3D-View of the Receiving Unit	65
Figure 3.36 The Block Diagram of the Experimental Setup	67
Figure 3.37 The Flow Chart of the Experimental Codes	68
Figure 3.38 The LED/PWM Indicator Sub-Block	69
Figure 3.39 PWM Control Sub-Block	69
Figure 3.40 Updating the Mode Selection Sub-Block	70
Figure 3.41 Updating the Generation Frequency Sub-Block	71
Figure 4.1 Power Transfer Against Coupling Coefficient Plot of Series-to-Series	76
Figure 4.2 Power Transfer Against Coupling Coefficient Plot of Series-to-Parallel	77
Figure 4.3 Power Transfer Against Coupling Coefficient Plot of Parallel-to-Series	77
Figure 4.4 Power Transfer Against Coupling Coefficient Plot of Parallel-to-Parallel	78
Figure 4.5 Power Transfer Against Coupling Coefficient Plot of All Configurations	79
Figure 4.6 Input Impedance Against the Frequency of Different Coupling Coefficient	82
Figure 4.7 Calculated and Simulated Input Impedance Against the Coupling Coefficient	83
Figure 4.8 Graph of Power Transfer Efficiency at Load Impedance of 10 Ω	84
Figure 4.9 Graph of Power Transfer Efficiency at Load Impedance of 50 Ω	85

Figure 4.10 Graph of Power Transfer Efficiency at Load Impedance of 100Ω	85
Figure 4.11 Graph of Optimum Load Impedance Versus Coupling Coefficient	88
Figure 4.12 Graph of Power Transfer Efficiency at the Optimum Load Impedance	88
Figure 4.13 The Experimental Set-Up of the Developed Hardware	89
Figure 4.14 Transmitted and Received Signal at 30kHz	90
Figure 4.15 The Portion of the Signal at 30kHz is Analyzed by MATLAB	91
Figure 4.16 Transmitted and Received Signal at 50kHz	91
Figure 4.17 The Portion of the Signal at 50kHz is Analyzed by MATLAB	92
Figure 4.18 Transmitted and Received Signal at 70kHz	92
Figure 4.19 The Portion of the Signal at 70kHz is Analyzed by MATLAB	93
Figure 4.20 Transmitted and Received Signal at 74.06kHz	93
Figure 4.21 The Portion of the Signal at 74.06kHz is Analyzed by MATLAB	94
Figure 4.22 Transmitted and Received Signal at 80kHz	94
Figure 4.23 The Portion of the Signal at 80kHz is Analyzed by MATLAB	95
Figure 4.24 Transmitted and Received Signal at 100kHz	95
Figure 4.25 The Portion of the Signal at 100kHz is Analyzed by MATLAB	96
Figure 4.26 Transmitted and Received Signal at 120kHz	96
Figure 4.27 The Portion of the Signal at 120kHz is Analyzed by MATLAB	97
Figure 4.28 Input and Output Waveforms at 30kHz – 0cm Apart	99
Figure 4.29 Input and Output Waveforms at 50kHz – 0cm Apart	99
Figure 4.30 Input and Output Waveforms at 58.4kHz – 0cm Apart	100
Figure 4.31 Input and Output Waveforms at 60kHz – 0cm Apart	100
Figure 4.32 Input and Output Waveforms at 70kHz – 0cm Apart	101
Figure 4.33 Input and Output Waveforms at 80kHz – 0cm Apart	101

Figure 4.34 Input and Output Waveforms at 90kHz – 0cm Apart	102
Figure 4.35 Input and Output Waveforms at 120kHz – 0cm Apart	102
Figure 4.36 Input and Output Waveforms at 30kHz – 2.54cm Apart	103
Figure 4.37 Input and Output Waveforms at 50kHz – 2.54cm Apart	104
Figure 4.38 Input and Output Waveforms at 60kHz – 2.54cm Apart	104
Figure 4.39 Input and Output Waveforms at 70kHz – 2.54cm Apart	105
Figure 4.40 Input and Output Waveforms at 75.1kHz – 2.54cm Apart	105
Figure 4.41 Input and Output Waveforms at 80kHz – 2.54cm Apart	106
Figure 4.42 Input and Output Waveforms at 90kHz – 2.54cm Apart	106
Figure 4.43 Input and Output Waveforms at 120kHz – 2.54cm Apart	107
Figure 4.44 Input and Output Waveforms at 0cm Apart – 57.88kHz	109
Figure 4.45 Input and Output Waveforms at 1cm Apart – 57.88kHz	109
Figure 4.46 Input and Output Waveforms at 2cm Apart – 57.88kHz	110
Figure 4.47 Input and Output Waveforms at 3cm Apart – 57.88kHz	110
Figure 4.48 Input and Output Waveforms at 4cm Apart – 57.88kHz	111
Figure 4.49 Input and Output Waveforms at 5cm Apart – 57.88kHz	111
Figure 4.50 Input and Output Waveforms at 0cm Apart – 71.18kHz	112
Figure 4.51 Input and Output Waveforms at 1cm Apart – 71.18kHz	112
Figure 4.52 Input and Output Waveforms at 2cm Apart – 71.18kHz	113
Figure 4.53 Input and Output Waveforms at 3cm Apart – 71.18kHz	113
Figure 4.54 Input and Output Waveforms at 4cm Apart – 71.18kHz	114
Figure 4.55 Input and Output Waveforms at 5cm Apart – 71.18kHz	114
Figure 4.56 Input and Output Waveforms at 0cm Apart – at Resonance	116
Figure 4.57 Input and Output Waveforms at 0.5cm Apart – at Resonance	117

Figure 4.58 Input and Output Waveforms at 1cm Apart – at Resonance	117
Figure 4.59 Input and Output Waveforms at 1.5cm Apart – at Resonance	118
Figure 4.60 Input and Output Waveforms at 2cm Apart – at Resonance	118
Figure 4.61 Input and Output Waveforms at 2.5cm Apart – at Resonance	119
Figure 4.62 Graph of V_{RMS} Delivered to the Output	122
Figure 4.63 Graph of Power Delivered to the Output	123
Figure 4.64 Graph of Power Received Ratio at Resonance Frequency to Two Arbitrarily Selected Frequencies	124
Figure 5.1 Proposed Block Diagram for Future Works	131



LIST OF ABBREVIATIONS

AC	Alternating Current
CT	Circuit Theory
DC	Direct Current
DFT	Discrete Fourier Transform
FFT	Fast Fourier Transform
IHD	Individual Harmonic Distortion
IPT	Inductive Power Transfer
KCL	Kirchhoff's Current Law
KVL	Kirchhoff's Voltage Law
PF	Power Factor
PP	Parallel-to-Parallel
PS	Parallel-to-Series
PWM	Pulse Width Modulation
RMS	Root Mean Square
SP	Series-to-Parallel
SS	Series-to-Series
THD	Total Harmonic Distortion
WPT	Wireless Power Transfer

LIST OF SYMBOLS

avg	Average
C	Capacitance
C_p	Primary Capacitor
C_s	Secondary Capacitor
I	Current
k	Coupling Coefficient
L	Inductance
L_p	Primary Inductor
L_s	Secondary Inductor
P_{rms}	Root Means Square Power
R_x	Resistor X
V_{rms}	Root Means Square Voltage
V_s	Input Voltage
V_o	Output Voltage
W	Watt
Z_{in}	Input Impedance
Z_{out}	Output Impedance

CHAPTER ONE

INTRODUCTION

1.1 BACKGROUND OF STUDY

In general, the concept of energy transfer through an air gap is not a new piece of new knowledge. Historically, it has been around since humans knew that magnetic coils could be used to induce an electric field. The term wireless power transfer (WPT) which is used to describe the technology to transfer energy/power to an electric load without having physical contact or medium, has been experimented with by Nicolas Tesla in the late 19th century through conducting several experiments (Shidujaman, Samani, & Arif, 2014). For example, Nicola tesla set up a large laboratory in Manhattan to conduct further experiments to realize his dream of supplying megawatt power wirelessly to ships without the need for a physical cable. He had raised a huge tower bearing a coil to provide power to the ship without requiring the ship to approach the shipyard. Unfortunately, studies in this area have been almost forgotten since Tesla's death, and some failed experiments by some pioneering works appear in the period after Tesla's death. Although Tesla was very ambitious, his work did not get much attention at the time until recently research in wireless power transfer was given a new breath, with newer research directions and interests.

With the development of electric appliances and applications, research in the wireless power transfer area has become a popular area lately. In addition, the recent research on wireless power transfer has contributed to new dimensions and aspects in the field of contactless power transfer applications (X. Lu, Wang, Niyato, Kim, & Han, 2016). For example, Electric Vehicles, which are now a reality in the very near future

in metropolitan transportation, are transforming into the Park-and-Charge concept right away from now. Further, RFID and IoT devices are other areas, where passive device activation or battery charging via non-contact devices is an obvious area for wireless charging applications. Other applications of wireless power transfer are autonomous underwater vehicles, public transport, for example, monorail, industrial automation, and robot manipulation and maneuvering of autonomous objects and unmanned aerial vehicles. Similarly, powering devices buried in civil structures for monitoring the purpose of physical parameters or activation of implants for the measurement of biological or biomedical parameters are areas where wireless power transfer has proven to be the only means of application (S. R. Khan, Pavuluri, Cummins, & Desmulliez, 2020).

Inductive resonant wireless power transfer is one of the most popular areas of wireless power transfer research. However, one of the main challenges in inductive resonant WPT is the loss of energy on the way from the energy source to the target device. There is a lot of work reported to overcome or reduce power loss throughout power transmission. Work addressing research parameters such as coil design, geometry or shape, resonance frequency channel parameters, or the effect of gap separation in the form of coupling coefficients has been widely reported. On top of that, there are other works reported, for example, fine-tuning the primary or/and the secondary capacitor for tuning and conditioning reasons; fine-tuning the primary or/and the secondary coils; and load impedance matching, to name a few.

This research addresses the optimization of power transfer through resonance frequency adjustment as well as focuses on techniques on how the resonance frequency of the inductive resonant WPT link can be estimated through simpler implementation efforts. In other words, this research is about proposing, validating, and verifying

resonance frequency estimation techniques for inductive resonant wireless power transfer (WPT).

1.2 RESEARCH QUESTION

The inductive resonant wireless power transfer efficiency can be maximized by ensuring the operating frequency as close as possible to the secondary coil resonance frequency. If the system is at the resonance frequency of the secondary coil, then the quality factor (Q) of the system is high. This ensures that almost all power at the primary coil is transferred to the secondary coil. Therefore, the major research question of this research is about devising a technique to estimate the resonance frequency with accuracy, making it a reason for estimating the coupling coefficient (k) of the inductive resonant WPT link. The open research question is whether such a technique can be reliably used to estimate the resonance frequency of inductive resonant wireless power transfer. Will the technique in stand-alone mode prove sufficient or require other parameters in the association? Exploring this work onward will pave the way into areas of automatic resonance frequency tracking and self-tuning research activities.

1.3 RESEARCH PHILOSOPHY

In general, almost all inductive resonant wireless power transfers rely on the square waves generated to run the DC-to-DC network in the form of an H-bridge as the voltage source. The voltage source in the form of a square wave is injected into the transmitter unit mutually coupled with the receiver unit. Depending on the resistance and reactance of the inductive resonant WPT system, the transmitted voltage is the result of a square wave signal modified by the inductive resonant WPT link response. In general, the resulting transmitted voltage depends on the frequency of the square wave injected into the WPT link, as well as the resonance frequency of the WPT link. The operating frequency or period of the injected square wave should be kept close to the resonance

frequency of the WPT link to ensure that the source finding the chain of the device mounted on the receiving unit appears to be a purely resistive load. The objective of this thesis is to estimate the resonance frequency of inductive resonant wireless power transfer by analyzing the transmitted voltage. Initially, total harmonics distortion (THD), Crest Factor, and VRMS were suggested as parameters to be used in estimating resonance frequency.

1.4 RESEARCH HYPOTHESIS

The hypothesis of the research is:

"It is possible to develop a method to estimate the resonance frequency of inductive resonant wireless power transfer links."

The research hypothesis is based on:

- 1- Assuming an inductive resonant wireless power transfer link is like a bandpass filter.
- 2- Assuming the inductive resonant WPT link allows the frequency components within its passband and discriminates all other frequency components.
- 3- Assuming that the resonance frequency of the inductive resonant WPT link can be estimated by the frequency response of the transmitting voltage across its primary coil.

1.5 PROBLEM STATEMENTS

In the resonant inductive wireless power transfer system, the energy from the primary coil is transferred inductively through the air gap to the secondary coil. This is usually implemented with purposely designed transformers. As with a wired power transmission system, power transmission efficiency in a wireless power transfer system is highly dependent on the capability of energy delivered from the primary coil to the secondary coil. It has been observed that ensuring high power transmission efficiency

is one of the most popular branches of research in wireless power transfer technology as well as the most challenging field for researchers.

Several factors are affecting the amount of power delivered to load. The most prominent factor is the coupling coefficient between the two coils. In contrast to the conventional transformer, the WPT coils are placed apart or/and aligned at some angle orientation. The farther the secondary coil is from the primary coil, the lower the amount of magnetic flux produced by the primary coil cutting through the secondary coil (Q. Li & Liang, 2015). As a result, the lesser the coupling coefficient between the two coils and the lesser power is delivered to load. The situation is the same if the two coils are aligned at an angle, the power transfer is maximum if the coils are arranged coaxially with the plane of the coils parallel to each other.

Another factor influencing the amount of power transfer is the quality factor (Q) of the secondary resonant coil. Where the ratio of energy store to energy loss is determined by the system quality factor which in other words, active or effective power gets wasted due to the presence of reactive power. Therefore, the presence of reactive power in the system must be reduced to improve power transfer. One way to address this wastage of power is to use tuning capacitors coupled to coils on both sides. Therefore, power transfer can be maximized by ensuring that the inductive resonant WPT works at the resonance frequency determined by the inductive and capacitive elements of the system. In (W. Zhang & Mi, 2016), the resonance frequency of the system has been proven to be determined by the resonance frequency of the receiving coil. For these reasons, the resonance frequency of the primary and secondary coils is practically set to operate at the same frequency.

However, the resonance frequency of the WPT is not regulated primarily by the capacitance and inductance of the system. The resonance frequency of the WPT also